

University of Groningen

## Functional interactions between the subunits of the lactose transporter from *Streptococcus thermophilus*

Geertsma, ER; Duurkens, RH; Poolman, Berend; Duurkens, Ria H.

*Published in:*  
Journal of Molecular Biology

*DOI:*  
[10.1016/j.jmb.2005.04.047](https://doi.org/10.1016/j.jmb.2005.04.047)

**IMPORTANT NOTE: You are advised to consult the publisher's version (publisher's PDF) if you wish to cite from it. Please check the document version below.**

*Document Version*  
Publisher's PDF, also known as Version of record

*Publication date:*  
2005

[Link to publication in University of Groningen/UMCG research database](#)

*Citation for published version (APA):*

Geertsma, E. R., Duurkens, R. H., Poolman, B., & Duurkens, R. H. (2005). Functional interactions between the subunits of the lactose transporter from *Streptococcus thermophilus*. *Journal of Molecular Biology*, 350(1), 102-111. DOI: 10.1016/j.jmb.2005.04.047

**Copyright**

Other than for strictly personal use, it is not permitted to download or to forward/distribute the text or part of it without the consent of the author(s) and/or copyright holder(s), unless the work is under an open content license (like Creative Commons).

**Take-down policy**

If you believe that this document breaches copyright please contact us providing details, and we will remove access to the work immediately and investigate your claim.

*Downloaded from the University of Groningen/UMCG research database (Pure): <http://www.rug.nl/research/portal>. For technical reasons the number of authors shown on this cover page is limited to 10 maximum.*

# Functional Interactions between the Subunits of the Lactose Transporter from *Streptococcus thermophilus*

Eric R. Geertsma, Ria H. Duurkens and Bert Poolman\*

Department of Biochemistry  
Groningen Biomolecular  
Sciences and Biotechnology  
Institute, University of  
Groningen, Nijenborgh 4  
9747 AG, Groningen, The  
Netherlands

Although the quaternary state has been assessed in detail for only a few members of the major facilitator superfamily (MFS), it is clear that multiple oligomeric states are represented within the MFS. One of its members, the lactose transporter LacS from *Streptococcus thermophilus* assumes a dimeric structure in the membrane and *in vitro* analysis showed functional interactions between both subunits when proton motive force ( $\Delta p$ )-driven transport was assayed. To study the interactions in further detail, a covalent dimer was constructed consisting of in tandem fused LacS subunits. These covalent dimers, composed of active and completely inactive subunits, were expressed in *Escherichia coli*, and initial rates of  $\Delta p$ -driven lactose uptake and lactose counterflow were determined. We now show that also *in vivo*, both subunits interact functionally; that is, partial complementation of the inactive subunit was observed for both transport modes. Thus, both subunits interact functionally in  $\Delta p$ -driven uptake and in counterflow transport. In addition, analysis of in tandem fused LacS subunits containing one regulatory LacS-IIA domain showed that regulation is primarily an intramolecular event.

© 2005 Elsevier Ltd. All rights reserved.

**Keywords:** membrane transport protein; major facilitator superfamily; oligomeric state; quaternary structure; functional subunit interactions

\*Corresponding author

## Introduction

The major facilitator superfamily (MFS) forms the largest family of secondary transporters. Its members, found in all living organisms, catalyze the translocation of a variety of substrates among which are sugars, peptides, anions, cations and hydrophobic compounds. Most MFS proteins consist of 12  $\alpha$ -helical transmembrane-spanning segments (TMS) that are connected by loop regions ranging from a few amino acid residues to several dozens of residues.<sup>1</sup> Although data on functional and structural aspects of these proteins are produced at a great pace, information on the quaternary state(s) is scarce. For both the lactose transporter LacY<sup>2</sup> and the sugar-phosphate antiporter UhpT<sup>3</sup> from *Escherichia coli*, the monomeric unit is sufficient for transport, and earlier claims for LacY dimers are thought to be based on improper

experimentation and inaccurate data interpretation. For the anion-exchanger AE1<sup>4,5</sup> and glucose transporter GLUT1<sup>6</sup> from human, and the tetracycline transporter TetA<sup>7,8</sup> from *E. coli*, on the other hand, there is compelling evidence that these transporters form higher oligomeric structures, and functional interactions between the subunits of the oligomers have been shown.

For secondary transporters outside the MFS, oligomeric states higher than the monomer have been proposed (e.g. the Na<sup>+</sup>/H<sup>+</sup> antiporter NhaA<sup>9</sup> and the multidrug exporter AcrB<sup>10</sup> from *E. coli*, the Na<sup>+</sup>/glycine betaine symporter BetP<sup>11</sup> from *Corynebacterium glutamicum*, and the human glial glutamate transporter hEAAT2<sup>12,13</sup>). For most of these transporters, it remains to be determined whether functional interactions between subunits take place. Furthermore, in those cases where cooperativity between subunits has been shown, the role of the oligomeric structure in the mechanism of transport is still far from clear.

Members of the galactoside-pentoside-hexuronide transporter family (GPH family) of the MFS<sup>14</sup> are of pro- or eukaryotic origin and catalyze the transport of sugars and sugar

Abbreviations used: MFS, major facilitator superfamily; TMS, transmembrane-spanning segments; GPH, galactoside-pentoside-hexuronide transporter;  $\Delta p$ , proton motive force; DDM, *n*-dodecyl- $\beta$ -D-maltoside.

E-mail address of the corresponding author:  
b.poolman@rug.nl

derivatives in symport with cations.<sup>15,16</sup> These transporters consist of 12  $\alpha$ -helical transmembrane segments that span the membrane in a zig-zag fashion. Detailed analysis of the oligomeric state has been conducted only for the lactose transporter LacS from *Streptococcus thermophilus*, and this system forms a structural and functional dimer. For the xyloside transporter XylP from *Lactobacillus pentosus*, a dimeric structure has been reported. On the other hand, the projection structure of another GPH family member, the melibiose permease MelB from *E. coli*, does not comply with a dimeric state.<sup>17</sup>

Both XylP and LacS have been analyzed in the detergent-solubilized state using blue native gel electrophoresis and analytical ultracentrifugation, and shown to be in a dynamic monomer to dimer equilibrium.<sup>13,18</sup> The extent of dimerization could be manipulated by varying the detergent type or concentration. The membrane-embedded oligomeric state of XylP and LacS has been determined using freeze-fracture electron microscopy, which suggested that both proteins are present in the bilayer as dimers only.<sup>13,18</sup> Additional evidence for this dimeric state of LacS in the membrane came from saturation-transfer electron spin resonance studies.<sup>19</sup> Chemical cross-linking of cysteine substitution mutants of LacS *in situ* suggested that on the extracellular side of LacS, TMS V and VIII, and on the cytoplasmic side TMS VI and VII, are located near the centre of the LacS dimer.<sup>20</sup> By studying LacS heterodimers of active (LacS(C320A)) and (conditionally) inactive (LacS(E67C/C320A)) species in proteoliposomes, it has been shown that the subunits within the dimer cooperate.<sup>21</sup> Cooperativity was observed during lactose accumulation driven by the proton motive force ( $\Delta p$ ), but not for the lactose exchange mode of transport.

Within a LacS subunit, two domains can be discerned. The N-terminal membrane-embedded carrier domain catalyzes the translocation event. The C-terminal hydrophilic LacS-IIA domain, unique for the LacS subfamily within the GPH family,<sup>15</sup> is homologous to IIA<sup>Glc</sup> domains of the PEP phosphotransferase system and resides at the cytoplasmic face of the membrane. The LacS-IIA domain is not essential for transport, but serves a regulatory role. Phosphorylation of LacS-IIA by HPr(His~P) enables the domain to interact with the carrier domain and modulate the transport activity (our unpublished results).<sup>22,23</sup>

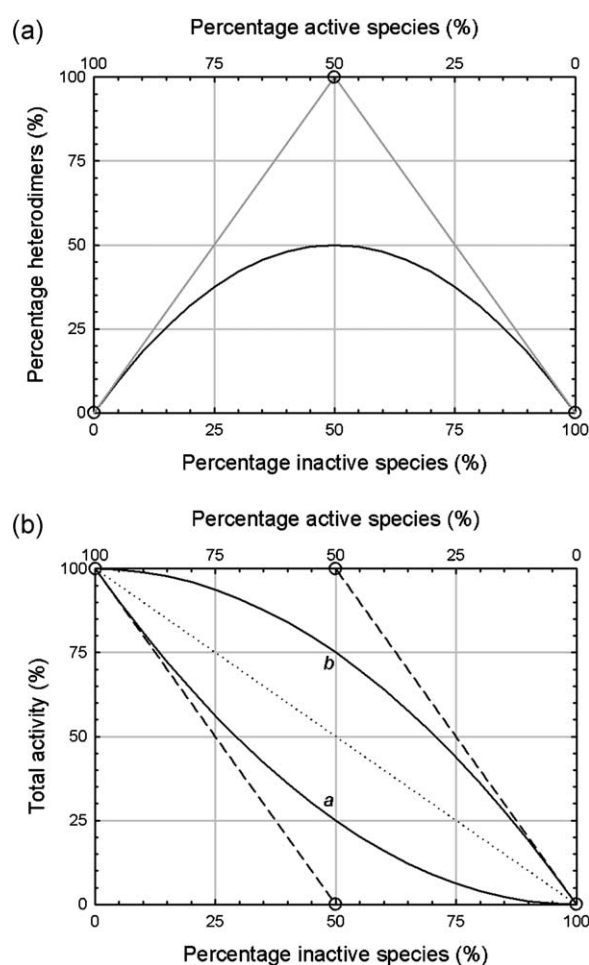
In order to increase our insights into the functional role(s) of the subunit interactions, heterodimers were formed by fusing two different LacS carrier domains in tandem. In whole *E. coli* cells, functional interactions between a LacS(D71C/C320A) subunit, which is inactive in all modes of transport but still adopts a conformation capable of substrate-binding,<sup>24</sup> and the active LacS(C320A) subunit were analyzed. In addition, the regu-

lation of the LacS carrier domain by LacS-IIA was studied in an asymmetric covalent dimer, in which only one subunit was equipped with a LacS-IIA domain.

## Results

### A covalent dimer to study subunit interactions

Functional interactions between subunits in



**Figure 1.** Comparison between the calculated amount of heterodimers and total activity for free and forced association of two species. (a) The black line depicts the percentage of heterodimers formed as a function of different ratios of active over inactive species, assuming random association. The circles connected by the gray line show the percentage of heterodimers if the subunits are covalently linked. (b) The summed activity of all species as a function of different ratios of active over inactive species. The dotted line represents the activity observed if the subunits function independently. Functional dominance of one type of subunit will lead to the continuous curves *a* and *b*, representing negative and positive dominance, respectively. Upon fusion of both subunits, these scenarios are represented by the circles connected by the broken lines. Note that for the forced association of the subunits, only three and no intermediate situations exist.

dimeric proteins have been studied by mixing active and inactive species in different ratios and characterizing the resulting heterodimers,<sup>21,25–27</sup> which constitute at most 50% of all dimers; that is, at an equal ratio of both species, as shown in Figure 1(a) (continuous line). If the association is random, each of the homodimers makes up 25% of all dimers at an equal ratio of both species. If two species do not interact or function independently, the total activity is determined only by the percentage of active species and will decrease linearly (Figure 1(b), dotted line). However, if both species do interact functionally and the phenotype of one of the species dominates the activity of the heterodimer, the activity will follow a quadratic relationship, as shown in Figure 1(b) (continuous lines); lines *a* and *b* are obtained when a subunit has a negative- or positive-dominant effect on the opposing subunit, respectively.

To determine if the subunits function in a cooperative manner, the specific activity of the heterodimer needs to be resolved. When the exact ratio of the two species is known (e.g. in a proteoliposomal system) this can be determined from the summed activity of all species. However, in whole cells, the ratio of two separately expressed subunits is difficult to control, because of variations in the expression and inaccuracies in the determination of protein levels from, for instance, immunoblots. By covalent coupling of subunits, the ratio is known beforehand, which has the additional advantage that the maximum percentage of heterodimers can be elevated from 50% to 100% (see Figure 1(a)). This increases the signal that discriminates between independent functioning and negative or positive-dominant effects of subunits, as shown in Figure 1(b).

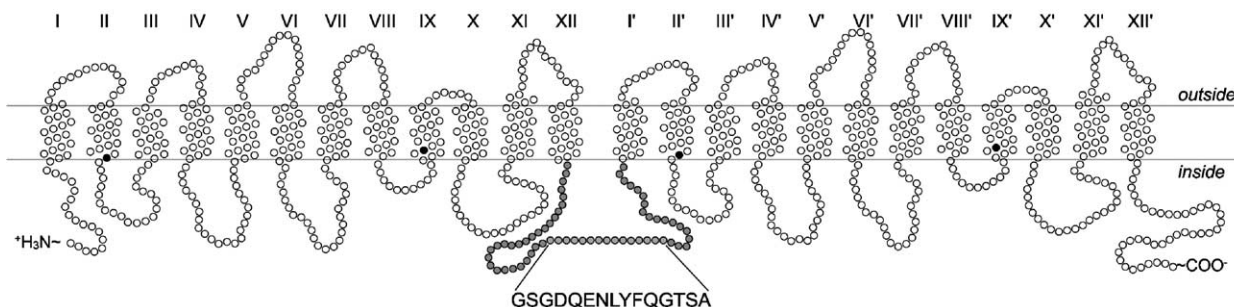
In order to control the total amount of protein in a reproducible way, expression of the covalent dimer in *E. coli* MC1061 was governed by the arabinose-inducible  $P_{BAD}$  promoter, which proved to be a more convenient and reliable expression system than the vector wherein LacS expression was controlled by its endogenous promoter (our unpublished results).

### Construction and functional expression of a covalent Lac $\Delta$ IIA<sub>2</sub> dimer

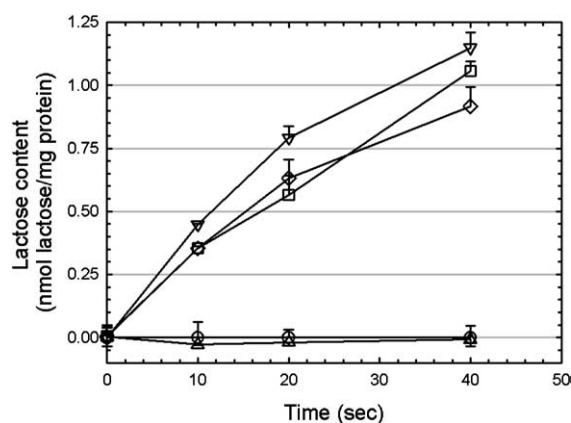
The minimal unit of LacS able to catalyze substrate translocation is the membrane-embedded carrier domain (our unpublished results).<sup>22</sup> To study the functional interactions of the carrier domains in a defined manner, the covalent LacS dimer comprised two joined Lac $\Delta$ IIA subunits rather than two LacS subunits. Lac $\Delta$ IIA lacks the C-terminal LacS-IIA domain that can be phosphorylated by HPr(His~P) (our unpublished results),<sup>22,23</sup> but shows equal rates of  $\Delta p$ -driven lactose transport and lactose counterflow as unphosphorylated full-length LacS (our unpublished results).

Twenty-eight amino acid residues follow the predicted end of TMS 12 of the first Lac $\Delta$ IIA(C320A) subunit. An artificial sequence of 15 amino acid residues was used to link the two subunits. At the DNA level, the linker region contains four endonuclease restriction sites and a sequence coding for a TEV protease recognition site, yielding the protein sequence GSGDQENLYFQGTSA. Together with the 18 amino acid residues preceding the predicted start of the first TMS of the second Lac $\Delta$ IIA(C320A) subunit, the total linker region connecting both subunits comprises 61 amino acid residues (Figure 2). This covalent dimer, in which both subunits contain the C320A mutation, was designated Lac $\Delta$ IIA<sub>2</sub>(CC).

As shown in Figure 3, Lac $\Delta$ IIA<sub>2</sub>(CC) catalyzed  $\Delta p$ -driven lactose uptake in whole *E. coli* MC1061 cells, demonstrating its functional expression and membrane insertion. Maximal transport activity of Lac $\Delta$ IIA<sub>2</sub> was observed when cells were induced with  $2 \times 10^{-3}\%$  (w/v) L-arabinose, whereas induction with  $1 \times 10^{-3}\%$  (w/v) L-arabinose yielded maximal transport activity of Lac $\Delta$ IIA (results not shown). At these optimal concentrations of inducer, the initial rates of  $\Delta p$ -driven lactose uptake for Lac $\Delta$ IIA<sub>2</sub>(CC) and Lac $\Delta$ IIA(C320A) were 2.6 nmol of lactose/mg of protein per minute and 11 nmol of lactose/mg of protein per minute, respectively. Analysis of the levels of Lac $\Delta$ IIA<sub>2</sub>



**Figure 2.** Topology model of the Lac $\Delta$ IIA<sub>2</sub> dimer. Membrane topology of the Lac $\Delta$ IIA subunits is based on the model of MelB.<sup>33</sup> The gray horizontal lines indicate the membrane interfaces. Asp71 in the second transmembrane segment (TMS) of each subunit is depicted in black. The Lac $\Delta$ IIA subunits are coupled *via* a linker of 61 amino acid residues (gray circles). The sequence of the artificially introduced stretch of 15 residues in the linker is shown. In all subunits, the endogenous Cys320 in TMS IX (also shown in black) was replaced by an alanine residue.



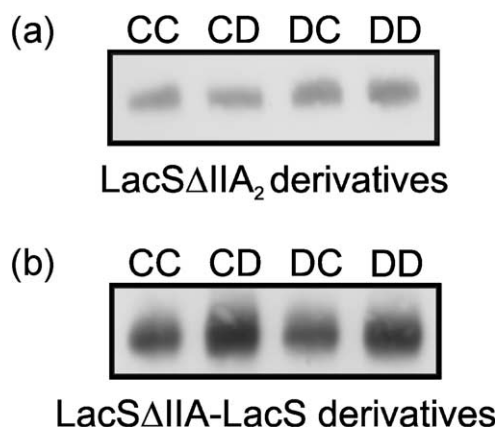
**Figure 3.**  $\Delta p$ -driven lactose transport by LacS $\Delta$ IIA<sub>2</sub> derivatives in *E. coli* MC1061. The accumulation of lactose driven by the proton motive force was measured in duplicate for LacS $\Delta$ IIA<sub>2</sub>(CC) (triangles pointing downwards), LacS $\Delta$ IIA<sub>2</sub>(CD) (squares), LacS $\Delta$ IIA<sub>2</sub>(DC) (triangles pointing upwards), LacS $\Delta$ IIA<sub>2</sub>(DD) (triangles pointing downwards), and MC1061 cells containing an empty plasmid with an ampicillin-resistance marker (pBluescript IISK+ (Stratagene)) (circles).

(CC) and LacS $\Delta$ IIA(C320A) showed that the former was indeed expressed several-fold lower (data not shown).

#### Inactive D71C/C320A subunits are complemented by active C320A subunits within LacS $\Delta$ IIA<sub>2</sub> during $\Delta p$ -driven and counterflow transport

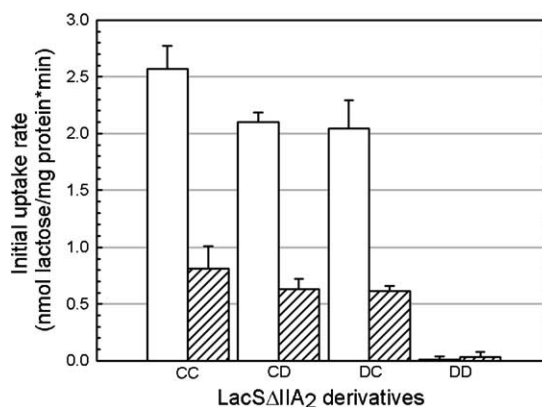
Heterodimeric LacS $\Delta$ IIA<sub>2</sub> derivatives were constructed, comprising the D71C mutation in either the first or the second subunit and using the C320A background. The D71C mutation renders LacS inactive in all modes of transport, but does not affect the overall structure of the transporter, as the capacity of LacS(D71C/C320A) to bind substrate was retained.<sup>24</sup> The LacS $\Delta$ IIA<sub>2</sub> derivatives containing the D71C/C320A mutation in the first, last, or both subunits were designated LacS $\Delta$ IIA<sub>2</sub>(DC), LacS $\Delta$ IIA<sub>2</sub>(CD), and LacS $\Delta$ IIA<sub>2</sub>(DD), respectively. The mutant variants of LacS $\Delta$ IIA<sub>2</sub> were expressed to comparable levels (Figure 4(a)), enabling a direct comparison of the transport activities.

Like the strain containing a control plasmid, cells expressing LacS $\Delta$ IIA<sub>2</sub>(DD) showed no significant uptake of lactose in whole *E. coli* MC1061 cells (Figure 3). The transport rates of LacS $\Delta$ IIA<sub>2</sub>(CD) and LacS $\Delta$ IIA<sub>2</sub>(DC) were equal, indicating that both halves of the forced dimer are correctly inserted in the membrane. The observed rates of  $\Delta p$ -driven lactose uptake of LacS $\Delta$ IIA<sub>2</sub>(CD) and LacS $\Delta$ IIA<sub>2</sub>(DC) were approximately 80% of the initial rate of uptake of LacS $\Delta$ IIA<sub>2</sub>(CC) (Figures 3 and 5). This result suggests that the D71C/C320A subunit is partially complemented by the active C320A subunit.



**Figure 4.** Immunoblots of covalently linked LacS derivatives, which were detected with an antibody directed against a hexa-His-tag. (a) Immunoblots of LacS $\Delta$ IIA<sub>2</sub> derivatives, purified from equal amounts of cells. CC and DD represent homodimers of C320A or D71C/C320A subunits, respectively. CD and DC represent heterodimers with a D71C/C320A subunit in the second or first subunit, respectively. (b) Immunoblots of the LacS $\Delta$ IIA-LacS derivatives, purified from equal amounts of cells. The same notation as that used in (a) indicates the different LacS $\Delta$ IIA-LacS derivatives.

Lactose counterflow transport by the LacS $\Delta$ IIA<sub>2</sub> derivatives showed a profile similar to that observed for  $\Delta p$ -driven lactose uptake (Figure 5). LacS $\Delta$ IIA<sub>2</sub>(DD) was completely defective in transport, and both



**Figure 5.** Initial rates of  $\Delta p$ -driven lactose uptake and lactose counterflow by LacS $\Delta$ IIA<sub>2</sub> derivatives in *E. coli* MC1061. Counterflow and  $\Delta p$ -driven lactose transport rates were measured on cell suspensions derived from the same culture. To measure lactose counterflow transport, de-energized cell suspensions were preloaded with 10 mM lactose and diluted into buffer containing 100  $\mu$ M [<sup>14</sup>C]lactose. Cells used to measure lactose transport driven by the  $\Delta p$  were pre-energized for two minutes by incubation with 10 mM D-Li-lactate and aeration. Subsequently, lactose accumulation was started by the addition of 50  $\mu$ M [<sup>14</sup>C]lactose. Each rate reflects the average from two independent experiments. Open and hatched bars reflect initial lactose uptake rates for  $\Delta p$ -driven and lactose counterflow transport, respectively.

LacS $\Delta$ IIA<sub>2</sub>(CD) and LacS $\Delta$ IIA<sub>2</sub>(DC) showed approximately 80% of the initial rate of lactose counterflow by LacS $\Delta$ IIA<sub>2</sub>(CC), indicating that for counterflow transport also the D71C/C320A subunit is partially complemented by the active C320A subunit.

### Covalent fusion of LacS $\Delta$ IIA subunits differently affects counterflow and $\Delta$ p-driven lactose transport










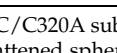
Under identical experimental conditions, non-covalently linked LacS(C320A) showed approximately half the rate of  $\Delta$ p-driven transport compared to lactose counterflow (9.0 nmol of lactose/mg of protein per minute and 20 nmol of lactose/mg of protein per minute, respectively), while LacS $\Delta$ IIA(C320A) showed comparable rates for both modes of transport (11 nmol of lactose/mg of protein per minute and 8.6 nmol of lactose/mg of protein per minute). This is most probably caused by a stimulation of the counterflow reaction of LacS(C320A) by HPr(His~P) mediated phosphorylation of LacS-IIA (our unpublished results).

Whereas the ratio of the initial rates of  $\Delta$ p-driven transport over counterflow was 0.5 and 1.3 for LacS and LacS $\Delta$ IIA, respectively, this ratio was approximately 3 for the CC, CD and DC derivatives of LacS $\Delta$ IIA<sub>2</sub> (summarized in Table 1). Since the initial rates of both  $\Delta$ p-driven and counterflow lactose transport were determined on cells derived from the same culture, the discrepancy in relative activities cannot be caused by variation in expression levels. Effects of variations in internal pH between both transport modes on

LacS $\Delta$ IIA<sub>2</sub> derivatives could be excluded, because the pH of the buffer during lactose counterflow transport was adjusted to 7.7, which was equal to the internal pH of cells during  $\Delta$ p-driven transport.<sup>28</sup> Furthermore, by charging the cells with [<sup>14</sup>C]lactose, it was shown that the MC1061 cells containing LacS $\Delta$ IIA<sub>2</sub> were equilibrated with lactose to levels similar to that of cells containing non-covalently linked LacS $\Delta$ IIA(C320A), ruling out limiting intracellular lactose concentrations as a cause for the decreased counterflow transport rates. We, therefore, conclude that the threefold difference in initial rates of  $\Delta$ p-driven lactose transport and lactose counterflow transport by the CC, CD, and DC derivatives of LacS $\Delta$ IIA<sub>2</sub> is a genuine property of these dimers.

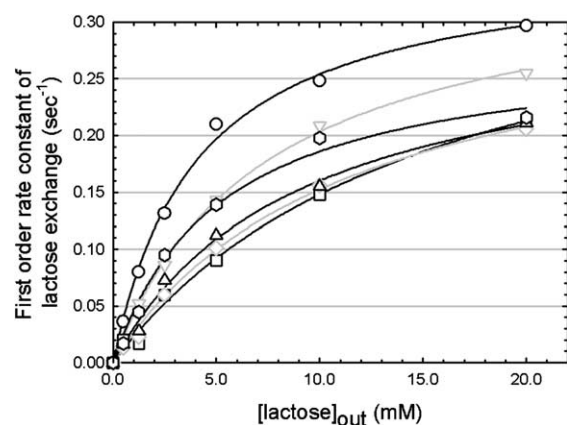
A more detailed kinetic analysis of lactose exchange transport, which comprises the same kinetics steps as counterflow transport and differs from counterflow only in substrate concentrations and the location of the <sup>14</sup>C isotope of lactose (inside for exchange, outside for counterflow), was conducted (Figure 6). All LacS $\Delta$ IIA<sub>2</sub> derivatives showed similar lactose exchange kinetics, again reflecting that all subunits (irrespective of the order of active C320A and inactive D71C/C320A subunits) were affected equally by the covalent linkage. Moreover, the apparent affinity constants of the LacS $\Delta$ IIA<sub>2</sub> derivatives for lactose were maximally increased only twofold compared to the  $K_m^{app}$  of LacS $\Delta$ IIA, suggesting that the overall structure of both subunits in the LacS $\Delta$ IIA<sub>2</sub> derivatives is conserved. Summarizing, it seems that both subunits within the LacS $\Delta$ IIA<sub>2</sub> derivatives adopt a correct conformation.

**Table 1.** Overview of the topology and transport rates of the LacS derivatives

LacS derivative	Topology	Initial transport rate (nmol lactose/mg protein per min) <sup>a</sup>		Ratio $\Delta$ p-driven/ counterflow
		$\Delta$ p-driven	Counterflow	
LacS(C320A)		9.04 ± 1.77	20.31 ± 0.53	0.45
LacS $\Delta$ IIA(C320A)		11.14 ± 0.59	8.59 ± 0.75	1.30
LacS $\Delta$ IIA <sub>2</sub> (CC)		2.57 ± 0.21 (100)	0.81 ± 0.20 (100)	3.17
LacS $\Delta$ IIA <sub>2</sub> (CD)		2.10 ± 0.08 (82)	0.63 ± 0.09 (78)	3.33
LacS $\Delta$ IIA <sub>2</sub> (DC)		2.04 ± 0.25 (79)	0.61 ± 0.05 (75)	3.34
LacS $\Delta$ IIA <sub>2</sub> (DD)		0.01 ± 0.03 (0)	0.03 ± 0.04 (4)	X
LacS $\Delta$ IIA-LacS(CC)		2.83 ± 0.35	4.51 ± 0.42	0.63
LacS $\Delta$ IIA-LacS(CD)		2.92 ± 0.29	1.73 ± 0.44	1.69
LacS $\Delta$ IIA-LacS(DC)		0.59 ± 0.21	0.93 ± 0.22	0.63
LacS $\Delta$ IIA-LacS(DD)		0.07 ± 0.08	0.11 ± 0.21	X

The LacS $\Delta$ IIA C320A and D71C/C320A subunit are presented as a rectangle, and a rectangle filled with a cross, respectively. The LacS-IIA domain is depicted as a flattened sphere. The initial transport rates were determined as described in the legend to Figure 5.

<sup>a</sup> Values within parentheses are percentages.

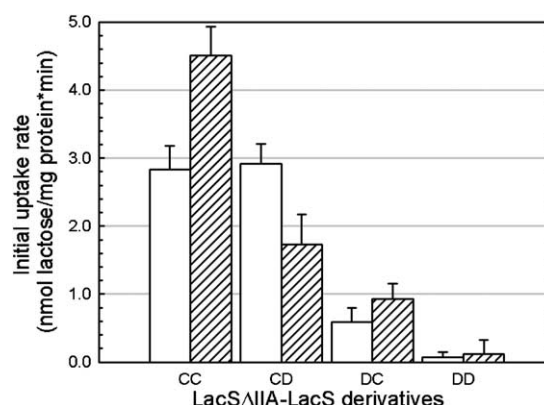


**Figure 6.** Kinetics of lactose exchange transport by LacS derivatives in *E. coli* MC1061. The initial rates of lactose exchange was measured for LacS (circles), LacS $\Delta$ IIA (triangles pointing downwards), LacS $\Delta$ IIA<sub>2</sub>(CC) (squares), LacS $\Delta$ IIA<sub>2</sub>(CD) (diamonds), LacS $\Delta$ IIA<sub>2</sub>(DC) (triangles pointing upwards), and LacS $\Delta$ IIA-LacS(CC) (hexagonals). Concentrated, de-energized cell suspensions were charged overnight with 5 mM [<sup>14</sup>C]lactose and the transport reaction was initiated by 100-fold dilution of the cells into KPM pH 7.7, supplemented with 50  $\mu$ M SF6847. The external lactose concentration varied from 50  $\mu$ M to 20 mM. To enable accurate determination of the kinetics of lactose exchange transport, cells expressing LacS or LacS $\Delta$ IIA were induced by a sevenfold lower concentration of L-arabinose than that used for counterflow and  $\Delta$ p-driven lactose transport. The exit of [<sup>14</sup>C]lactose from the cells was mono-exponential, and the half-time of the decay was used to calculate the first-order rate constant ( $k_{ex}$ ). The  $k_{ex}$  was plotted against the external lactose concentration and fit with the Michaelis-Menten equation.

### The LacS-IIA domain interacts primarily with the subunit of LacS $\Delta$ IIA-LacS to which it is attached

Upon HPr(His~P)-mediated phosphorylation of His552 in the LacS-IIA domain, the LacS-IIA domain interacts with the carrier and thereby stimulates lactose counterflow (our unpublished results).<sup>23</sup> To determine whether the regulation of the LacS-IIA domain occurs inter- or intramolecularly, a tandem fusion was constructed in which the last subunit has a C-terminal LacS-IIA domain attached to the carrier domain, creating a topology equal to the full-length LacS protein. This construct is designated LacS $\Delta$ IIA-LacS. The mutant variants derived from this construct, harboring the D71C mutation, were not expressed to an equal level, as shown in Figure 4(b). Constructs containing the D71C substitution in the second subunit were expressed to a higher level than subunits without a D71C mutation. This variation in expression levels allowed only a qualitative analysis, since exact quantification of the amount of functional transporters was not possible at this stage, due to the lack of a suitable ligand-binding assay.

The rate of  $\Delta$ p-driven lactose uptake of LacS $\Delta$ IIA-



**Figure 7.** Initial rates of  $\Delta$ p-driven lactose uptake and lactose counterflow by LacS $\Delta$ IIA-LacS derivatives in *E. coli* MC1061. Counterflow and  $\Delta$ p-driven lactose transport rates were measured on concentrated cell suspensions derived from the same culture as described in the legend to Figure 5. Each rate reflects the average from two independent experiments. Open and hatched bars reflect initial lactose uptake rates for  $\Delta$ p-driven and lactose counterflow transport, respectively.

LacS(CC) was in the same range as the rate of LacS $\Delta$ IIA<sub>2</sub>(CC) (2.8 nmol of lactose/mg protein per minute and 2.6 nmol of lactose/mg protein per minute, respectively) (Figure 7). Furthermore, the kinetics of lactose exchange by LacS $\Delta$ IIA-LacS(CC) yielded an apparent affinity constant for lactose similar to that of the other LacS derivatives (Figure 6). In line with the observations on the LacS $\Delta$ IIA<sub>2</sub> derivatives, both LacS $\Delta$ IIA-LacS(CD) and LacS $\Delta$ IIA-LacS(DC) were active in  $\Delta$ p-driven transport, whereas LacS $\Delta$ IIA-LacS(DD) was inactive (Figure 7).

As described above, the ratio of the initial rates of  $\Delta$ p-driven transport over counterflow was 0.5 and 1.3 for LacS and LacS $\Delta$ IIA, respectively, while this ratio was close to 3 for the CC, CD and DC derivatives of LacS $\Delta$ IIA<sub>2</sub> (summarized in Table 1). Both LacS $\Delta$ IIA-LacS derivatives that had a LacS-IIA domain attached to the active C320A subunit (LacS $\Delta$ IIA-LacS(CC) and LacS $\Delta$ IIA-LacS(DC)) showed a ratio of  $\Delta$ p-driven transport over counterflow of approximately 0.6. In contrast, this ratio was elevated to 1.7 for LacS $\Delta$ IIA-LacS(CD). Since the ratio differs for the LacS $\Delta$ IIA-LacS(CD) and LacS $\Delta$ IIA-LacS(DC) constructs, this suggests strongly that the IIA domain is restricted in its opportunity to interact with the carrier domains within the LacS dimer. Most likely, it cannot interact with any nearby subunit but only with the subunit to which it is attached.

## Discussion

Several independent studies led to the conclusion that the detergent-solubilized LacS protein is in monomer to dimer equilibrium,<sup>18,20,29</sup> whereas

membrane-embedded LacS is dimeric.<sup>18–20</sup> Veenhoff *et al.* showed by *in vitro* analysis of membrane-reconstituted (conditionally) inactive LacS(E67C/C320A) and active LacS(C320A) species that, within this structural dimer, functional interactions between the subunits take place in  $\Delta p$ -driven uptake but not in counterflow transport.<sup>21</sup> Here, we report the first *in vivo* demonstration of functional interactions between the subunits within the LacS dimer and show that both subunits functionally interact in  $\Delta p$ -driven transport and in counterflow. We show that: (i) the activity of the D71C mutant is (partially) restored by an active subunit; (ii) covalent linkage of two LacS subunits increases the rate of  $\Delta p$ -driven uptake relative to counterflow transport; and (iii) phosphorylation of the LacS-IIA domain stimulates the *cis* rather than the *trans* subunit of dimeric LacS.

Due to its uncoupled phenotype in whole cells, resulting in rapid efflux of lactose down the concentration gradient, LacS(E67C/C320A), previously used to demonstrate functional interactions within the LacS dimer *in vitro*,<sup>21</sup> could not be used to study subunit interactions in whole cells. Instead, the translocation-defective but lactose binding-competent LacS(D71C/C320A) was employed. Both Glu67 and Asp71 are located in TMS II, and acidic residues at these positions are highly conserved throughout the GPH family. Glu67 has been proposed to be involved in coupling proton and galactoside transport, whereas Asp71 is thought to contribute to the proton binding site.<sup>15</sup> In addition, both residues are in a region that is conformationally active upon substrate-binding.<sup>24</sup> Membrane-reconstituted LacS(E67C/C320A) catalyzes lactose counterflow transport at ~80% of the rate of LacS(C320A) and after modification of Cys67 with NEM ~30% activity remained. LacS(E67C/C320A) is completely defective in  $\Delta p$ -driven lactose transport.<sup>21</sup> In contrast, LacS(D71C/C320A) is inactive in both  $\Delta p$ -driven lactose transport and lactose counterflow, but the overall structure of the protein is retained as substrate-binding still occurs. Several second-site suppressor mutations of Cys71 have been isolated, among which R230C, which could restore lactose counterflow transport but not  $\Delta p$ -driven lactose transport.<sup>24</sup> By employing LacS(D71C/C320A) in tandem constructs with LacS(C320A), the effect of a subunit defective in all transport modes could be determined.

The Lac $\Delta$ IIA<sub>2</sub> derivatives were expressed functionally, although the levels were lower than those of the free subunits, as observed before for other in tandem fusion proteins.<sup>2,26</sup> The expression levels of the different Lac $\Delta$ IIA<sub>2</sub> derivatives were equal, as judged by immunoblotting (Figure 4(a)), but this technique lacks the sensitivity to demonstrate small variations (<20%) in expression levels. The Lac $\Delta$ IIA<sub>2</sub>(CC) was functional in both  $\Delta p$ -driven and lactose counterflow transport, and both subunits are membrane-inserted, as Lac $\Delta$ IIA<sub>2</sub>(CD) and Lac $\Delta$ IIA<sub>2</sub>(DC) showed similar transport rates. Lac $\Delta$ IIA<sub>2</sub>(DD), which resembles the

LacS(D71C/C320A) homodimer, is inactive, indicating that the mere coupling of the subunits is not sufficient for the restoration of the transport capacity. The difference in the ratio between the initial rates of  $\Delta p$ -driven lactose transport and lactose counterflow for the Lac $\Delta$ IIA<sub>2</sub> derivatives when compared with Lac $\Delta$ IIA and LacS, suggest that either  $\Delta p$ -driven lactose transport benefits or lactose counterflow activity deficits from the fusion of the subunits (Table 1). Kinetic analysis of lactose exchange transport showed that substrate-binding of the Lac $\Delta$ IIA<sub>2</sub> derivatives was affected only slightly, because the  $K_m^{app}$  was at most twofold higher than the  $K_m^{app}$  of the Lac $\Delta$ IIA dimer. Taken together, the covalent coupling of subunits introduces only some moderate changes within the LacS dimer and seems a valid system to study subunit interactions.

For independent operating subunits within the LacS dimer, the heterodimers Lac $\Delta$ IIA<sub>2</sub>(CD) and Lac $\Delta$ IIA<sub>2</sub>(DC) would be expected to show half the initial transport rates of Lac $\Delta$ IIA<sub>2</sub>(CC). A negative dominant phenotype of the D71C subunit would yield inactive Lac $\Delta$ IIA<sub>2</sub>(CD) and Lac $\Delta$ IIA<sub>2</sub>(DC) heterodimers. Clearly, both scenarios do not apply, since the initial rates of Lac $\Delta$ IIA<sub>2</sub>(CD) and Lac $\Delta$ IIA<sub>2</sub>(DC) for both  $\Delta p$ -driven lactose transport and lactose counterflow were approximately 80% of the rates of Lac $\Delta$ IIA<sub>2</sub>(CC) (Table 1). Rather, these transport activities support the contention that the C320A subunit has a positive-dominant effect, since it is able to partly restore the activity of the Lac $\Delta$ IIA(D71C/C320A) subunit.

Our new findings differ in some aspects from previous observations, using a proteoliposomal system, which demonstrated functional interactions between the LacS subunits for  $\Delta p$ -driven lactose transport only.<sup>21</sup> In proteoliposomes, increasing the percentage of impaired LacS(E67C/C320A) over LacS(C320A) resulted in a linear decrease in lactose counterflow transport, suggesting that the subunits function independently during this mode of transport. Furthermore, heterodimers composed of inactive LacS(E67C/C320A) and active LacS(C320A) were shown to be completely inactive in  $\Delta p$ -driven lactose transport, indicating negative dominance of the LacS(E67C/C320A) subunit. In the present study, negative dominance of the Lac $\Delta$ IIA(D71C/C320A) subunit in Lac $\Delta$ IIA<sub>2</sub>(CD) or (DC), is clearly not observed. Rather than interpreting these discrepancies in terms of differences in the experimental context (proteoliposomes *versus* intact cells), we feel that they can be explained by the different phenotypes of the LacS(E67C/C320A) and LacS(D71C/C320A) mutants. Most likely, LacS(D71C/C320A) is locked in one conformation, since it has lost its ability to reorient its substrate-binding sites as required for transport while retaining the ability to bind substrate.<sup>24</sup> An opposing functional subunit could enable the Lac $\Delta$ IIA(D71C/C320A) to overcome this locked conformation, leading to (partial) complementation. LacS(E67C/C320A), on the other hand, kept the ability to reorient its binding sites



and thereby catalyze lactose counterflow transport. Only its ability to catalyze  $\Delta p$ -driven lactose transport was impaired. As the extent of the impairment is different for both mutants, this may explain the lack of complementation of LacS(E67C/C320A) by LacS(C320A).

Apart from the relative activities of the different LacS $\Delta$ IIA<sub>2</sub> derivatives for either  $\Delta p$ -driven lactose uptake or lactose counterflow, the ratio of the initial rates of  $\Delta p$ -driven lactose transport over counterflow reveals interesting features. This ratio is approximately 3 for the CC, CD and DC derivatives of LacS $\Delta$ IIA<sub>2</sub>, while it is close to 1 for LacS $\Delta$ IIA. It is likely that the difference in the ratio of the initial rates for LacS $\Delta$ IIA<sub>2</sub> compared to LacS $\Delta$ IIA is a specific property of the fusion protein, caused by the presence of the linker connecting both subunits. A possible consequence of the covalent coupling could be the decreased ability of the subunits to separate transiently.

Additionally, the mere presence of the LacS-IIA domain to the second subunit decreased the ratio of  $\Delta p$ -driven transport over counterflow from  $\sim 3$  to 0.6–1.7, indicating that phosphorylation of this domain affects the subunit interactions. Since the absolute rates of  $\Delta p$ -driven lactose transport of LacS $\Delta$ IIA<sub>2</sub>(CC) and LacS $\Delta$ IIA-LacS(CC) are similar, it seems that the rate of lactose counterflow transport is increased upon addition of the LacS-IIA domain. Therefore, it is tempting to speculate that the kinetic step that is impaired by the coupling of the subunits is the same as the one that is stimulated by the phosphorylation of the LacS-IIA domain. Thus, the phosphorylated LacS-IIA domain could induce a transient conformation of the carrier domain that is less strongly interacting with the opposing subunit.

Under the conditions used, the IIA-domain of LacS is phosphorylated in *E. coli* MC1061, resulting in an increase in the rate of counterflow transport and a decrease in the ratio of  $\Delta p$ -driven transport over counterflow (our unpublished results). Phosphorylation of the LacS-IIA domain in the LacS $\Delta$ IIA-LacS derivatives resulted in a ratio of  $\Delta p$ -driven transport over counterflow near 0.6 if the LacS-IIA domain was associated with the LacS $\Delta$ IIA(C320A) subunit (Figure 7), and near 1.7 if it was associated with the inactive D71C subunit. The difference in the ratio of both transport modes observed for LacS $\Delta$ IIA-LacS(CD) and LacS $\Delta$ IIA-LacS(DC) suggests that the LacS-IIA domain prefers to functionally interact with the subunit to which it is attached. Although the rate of lactose counterflow is increased relatively for LacS $\Delta$ IIA-LacS(CD), the increase is smaller than that observed for the CC and DC derivatives of LacS $\Delta$ IIA-LacS, indicating that the D71C/C320A subunit cannot be stimulated by phosphorylated LacS-IIA to the same extent as the C320A subunit.

Taken together, the data presented here strengthen the conclusion that the two subunits of the LacS dimer interact functionally, as separate proteins *in vitro* and in tandem fusions *in vivo*. The

functional interactions within the LacS dimer take place during both  $\Delta p$ -driven lactose transport and lactose counterflow, and can be both positive and negative of nature. Furthermore, the LacS-IIA domain primarily stimulates transport through intramolecular interactions with the carrier domain.

## Materials and Methods

### Bacterial strain

*E. coli* JM110<sup>30,31</sup> was used for intermediate cloning steps. The final constructs were expressed in *E. coli* MC1061 (relevant genotype:  $\Delta lacZY, araBAD C^-$ ).<sup>32</sup> Both strains were cultivated at 37 °C on Luria broth under vigorous aeration. When appropriate, the medium was supplemented with 50  $\mu$ g/ml of ampicillin.

### Plasmid constructions

DNA manipulations were done according to standard protocols. The construction of pBADlacSC320A, pSKE8EhisC320A-BamH1-IIA, pNlacSC320Ahis and pSKlacSC320A $\Delta$ IIA will be described elsewhere. Plasmids pSKE8EhisC320A and pSKE8EhisC320A/D71C have been described.<sup>24</sup>

#### *pSKlacSC320A/D71C $\Delta$ IIA*

The NcoI-XhoI fragment of pSKlacSC320A $\Delta$ IIA was replaced by the 2147 bp NcoI-XhoI fragment from pSKE8EhisC320A/D71C.

#### *pBADlac $\Delta$ IIAlac $\Delta$ IIA*

In order to incorporate the D71C mutation in the first subunit, the 200 bp AatII-NcoI fragment from pSKE8EhisC320A-BamH1-IIA was replaced by the AatII-NcoI fragment from pSKE8EhisC320A/D71C, yielding pSKE8EhisC320A/D71C-BamH1-IIA. Plasmid pSKE8EhisC320A(/D71C)-BamH1-IIA was digested with BamH1-SpeI and ligated to a linker of two annealed oligonucleotides (linkerBS and linkerSB; see Table 2) with extensions resembling a BamH1 or an SpeI overhang. The AatII-XbaI fragment of this product was ligated into AatII-XbaI-digested pBADlacSC320A, yielding pBADsub1C320A(/D71C).

In order to construct the plasmid containing the second subunit, pNlacSC320Ahis was digested with BclI-NcoI and the 389 bp fragment was replaced by a linker of two annealed oligonucleotides (linkerBN and linkerNB; see Table 2) with extensions resembling a BclI or an NcoI overhang, yielding pBADsub2C320A+IIA. The sequence coding for the LacS-IIA-domain was removed by exchange of the 2229 bp AatII-XbaI fragment for the 1723 bp AatII-XbaI fragment from pSKlacSC320A(/D71C) $\Delta$ IIA, producing pBADsub2C320A(/D71C) $\Delta$ IIA.

To link both subunits, the 34 bp BclI-XbaI fragment from pBADsub1C320A(/D71C) was exchanged for the 2333 bp BclI-XbaI fragment from pBADsub2C320A(/D71C) $\Delta$ IIA containing the second subunit, yielding pBADlac $\Delta$ IIAlac $\Delta$ IIA. Four derivatives of pBADlac $\Delta$ IIAlac $\Delta$ IIA were generated, containing the D71C mutation in the first, the last, or both subunits.

**Table 2.** The complementary oligonucleotides constituting parts of the linker connecting both LacS-carrier domains

Primer	Sequence
LinkerBS	5'/gatccggtgatcaggagaacctctattttcaaggca
LinkerSB	5'/ctagtgcttgaaaatagaggttctctgatcaccg
LinkerBN	5'/gatcaggagaacctctattttcaaggcactagtgc
LinkerNB	5'/catggcactagtgccttgaaaatagaggttctct

LinkerBS and LinkerSB constitute a double-stranded linker with artificial BamHI and SpeI overhangs. LinkerBN and LinkerNB constitute a double-stranded linker with artificial BclI and NcoI overhangs. The sequence of both double-stranded linkers partially overlaps; double-stranded linkers were created by mixing both oligonucleotides in equal ratios, boiling for five minutes and annealing by cooling slowly to room temperature.

### pBADlacSΔIIA/lacS+IIA

The construction of the vector harboring a gene coding for a fusion between a LacS carrier domain and full-length LacS was similar to the construction of the vector for two fused LacS carrier domains. Instead of pBADsub2C320A(/D71C)ΔIIA, plasmid pBADsub2C320A(/D71C)+IIA was used. The D71C mutation was added by exchanging the 2229 bp AatII-XbaI fragment of pBADsub2C320A+IIA for the 2229 bp AatII-XbaI fragment of pSKE8EhisC320A/D71C.

### Whole cell transport assays

#### Cultivation

*E. coli* MC1061 cells were cultivated, washed and concentrated as will be described elsewhere. Cultures were induced with  $1 \times 10^{-3}$  % and  $2 \times 10^{-3}$  % (w/v) L-arabinose when LacS derivatives or LacS–LacS fusion proteins were expressed, respectively. Cells used for lactose exchange transport were induced with  $1.5 \times 10^{-4}$  % (w/v) L-arabinose when LacS or LacSΔIIA were expressed. Concentrated cell preparations were kept on ice until lactose transport was assayed.

#### Transport assays

General handlings involved in lactose transport in *E. coli* MC1061 cells and the preparation of cells to be used for Δp-driven lactose uptake and lactose counterflow transport will be described elsewhere.

#### Lactose exchange transport

Cells were concentrated to 45 mg protein/ml and incubated overnight in KPM (50 mM KPi (pH 7.7), 2 mM MgSO<sub>4</sub>) plus 5 mM [<sup>14</sup>C]lactose. The next day, cells were de-energized by incubation with the protonophore SF6847 (50 μM) plus 30 mM NaN<sub>3</sub> for two hours. Lactose exchange was assayed at 20 °C by 100-fold dilution of the cells into KPM, supplemented with 50 μM SF6847. The external lactose concentration varied from 50 μM to 20 mM.

#### Membrane vesicle isolation

Inside-out membrane vesicles from *E. coli* MC1061 cells were prepared as described.<sup>20</sup> Membrane vesicles were resuspended in 50 mM KPi (pH 7), plus 3 mM DTT, frozen in liquid nitrogen and stored at –80 °C. The protein concentration was determined using the DC protein assay (Bio-Rad).

### Purification and immunodetection of LacS–LacS fusion proteins

All steps during the purification were performed at 4 °C. *E. coli* MC1061 membrane vesicles (approximately 6 mg of total protein) containing LacS fusion proteins were deprived of DTT by washing and subsequently solubilized as described.<sup>20</sup> Next, the insoluble fraction was removed by centrifugation at 267,000 g for 15 minutes) and the supernatant was mixed with 0.25 ml of Ni-NTA resin that was washed with ten volumes of MilliQ water and two volumes of elution buffer (200 mM imidazole (pH 7.0), 10% (v/v) glycerol) and pre-equilibrated with four volumes of solubilization buffer (15 mM imidazole (pH 8.0), 100 mM NaCl, 10% (v/v) glycerol) supplemented with 0.05% (w/v) DDM. The mixture was incubated for one hour with continuous mixing. After that, the column was drained, washed with 30 volumes of solubilization buffer plus 0.05% DDM and eluted with elution buffer plus 0.05% DDM.

Samples were analysed by SDS-PAGE, semi-dry electroblotting and subsequent immunodetection with a primary antibody directed against a hexa-His-tag (Amersham Pharmacia Biotech) as described.<sup>20</sup>

### Acknowledgements

E.R.G acknowledges J. H. A. Folgering and L. M. Veenhoff for helpful discussions and the EU-FP6 programme (E-Mep; 504601) for funding.

### References

1. Pao, S. S., Paulsen, I. T. & Saier, M. H., Jr (1998). Major facilitator superfamily. *Microbiol. Mol. Biol. Rev.* **62**, 1–34.
2. Sahin-Toth, M., Lawrence, M. C. & Kaback, H. R. (1994). Properties of permease dimer, a fusion protein containing two lactose permease molecules from *Escherichia coli*. *Proc. Natl Acad. Sci. USA*, **91**, 5421–5425.
3. Ambudkar, S. V., Anantharam, V. & Maloney, P. C. (1990). UhpT, the sugar phosphate antiporter of *Escherichia coli*, functions as a monomer. *J. Biol. Chem.* **265**, 12287–12292.
4. Dahl, N. K., Jiang, L., Chernova, M. N., Stuart-Tilley, A. K., Shmukler, B. E. & Alper, S. L. (2003). Deficient HCO<sub>3</sub><sup>-</sup> transport in an AE1 mutant with normal Cl<sup>-</sup> transport can be rescued by carbonic anhydrase II presented on an adjacent AE1 protomer. *J. Biol. Chem.* **278**, 44949–44958.

5. Taylor, A. M., Zhu, Q. & Casey, J. R. (2001). Cysteine-directed cross-linking localizes regions of the human erythrocyte anion-exchange protein (AE1) relative to the dimeric interface. *Biochem. J.* **359**, 661–668.
6. Zottola, R. J., Cloherty, E. K., Coderre, P. E., Hansen, A., Hebert, D. N. & Carruthers, A. (1995). Glucose transporter function is controlled by transporter oligomeric structure. A single, intramolecular disulfide promotes GLUT1 tetramerization. *Biochemistry*, **34**, 9734–9747.
7. Yin, C. C., ma-Ramos, M. L., Borges-Walmsley, M. I., Taylor, R. W., Walmsley, A. R., Levy, S. B. & Bullough, P. A. (2000). The quarternary molecular architecture of TetA, a secondary tetracycline transporter from *Escherichia coli*. *Mol. Microbiol.* **38**, 482–492.
8. Hickman, R. K. & Levy, S. B. (1988). Evidence that TET protein functions as a multimer in the inner membrane of *Escherichia coli*. *J. Bacteriol.* **170**, 1715–1720.
9. Gerchman, Y., Rimon, A., Venturi, M. & Padan, E. (2001). Oligomerization of NhaA, the Na<sup>+</sup>/H<sup>+</sup> antiporter of *Escherichia coli* in the membrane and its functional and structural consequences. *Biochemistry*, **40**, 3403–3412.
10. Murakami, S., Nakashima, R., Yamashita, E. & Yamaguchi, A. (2002). Crystal structure of bacterial multidrug efflux transporter AcrB. *Nature*, **419**, 587–593.
11. Ziegler, C., Morbach, S., Schiller, D., Kramer, R., Tziatzios, C., Schubert, D. & Kuhlbrandt, W. (2004). Projection structure and oligomeric state of the osmoregulated sodium/glycine betaine symporter BetP of *Corynebacterium glutamicum*. *J. Mol. Biol.* **337**, 1137–1147.
12. Gendreau, S., Voswinkel, S., Torres-Salazar, D., Lang, N., Heidtmann, H., tro-Dassen, S. *et al.* (2004). A trimeric quaternary structure is conserved in bacterial and human glutamate transporters. *J. Biol. Chem.* **279**, 39505–39512.
13. Veenhoff, L. M., Heuberger, E. H. M. L. & Poolman, B. (2002). Structure and mechanism of the lactose permease of *Escherichia coli*. *Trends Biochem. Sci.* **27**, 242–249.
14. Saier, M. H., Jr (2000). Families of transmembrane sugar transport proteins. *Mol. Microbiol.* **35**, 699–710.
15. Poolman, B., Knol, J., van der Does, C., Henderson, P. J., Liang, W. J., Leblanc, G. *et al.* (1996). Cation and sugar selectivity determinants in a novel family of transport proteins. *Mol. Microbiol.* **19**, 911–922.
16. Reinders, A. & Ward, J. M. (2001). Functional characterization of the alpha-glucoside transporter Sut1p from *Schizosaccharomyces pombe*, the first fungal homologue of plant sucrose transporters. *Mol. Microbiol.* **39**, 445–454.
17. Hacksell, I., Rigaud, J. L., Purhonen, P., Pourcher, T., Hebert, H. & Leblanc, G. (2002). Projection structure at 8 Å resolution of the melibiose permease, an Na-sugar co-transporter from *Escherichia coli*. *EMBO J.* **21**, 3569–3574.
18. Friesen, R. H. E., Knol, J. & Poolman, B. (2000). Quaternary structure of the lactose transport protein of *Streptococcus thermophilus* in the detergent-solubilized and membrane-reconstituted state. *J. Biol. Chem.* **275**, 33527–33535 and 40658, correction.
19. Spooner, P. J., Friesen, R. H. E., Knol, J., Poolman, B. & Watts, A. (2000). Rotational mobility and orientational stability of a transport protein in lipid membranes. *Biophys. J.* **79**, 756–766.
20. Geertsma, E. R., Duurkens, R. H. & Poolman, B. (2003). Identification of the dimer interface of the lactose transport protein from *Streptococcus thermophilus*. *J. Mol. Biol.* **332**, 1165–1174.
21. Veenhoff, L. M., Heuberger, E. H. M. L. & Poolman, B. (2001). The lactose transport protein is a cooperative dimer with two sugar translocation pathways. *EMBO J.* **20**, 3056–3062.
22. Poolman, B., Knol, J., Mollet, B., Nieuwenhuis, B. & Sulter, G. (1995). Regulation of bacterial sugar-H<sup>+</sup> symport by phosphoenolpyruvate-dependent enzyme I/HPr-mediated phosphorylation. *Proc. Natl Acad. Sci. USA*, **92**, 778–782.
23. Gunnewijk, M. G. W. & Poolman, B. (2000). HPr(His~P)-mediated phosphorylation differently affects counterflow and proton motive force-driven uptake *via* the lactose transport protein of *Streptococcus thermophilus*. *J. Biol. Chem.* **275**, 34080–34085.
24. Veenhoff, L. M., Geertsma, E. R., Knol, J. & Poolman, B. (2000). Close approximation of putative alpha-helices II, IV, VII, X, and XI in the translocation pathway of the lactose transport protein of *Streptococcus thermophilus*. *J. Biol. Chem.* **275**, 23834–23840.
25. Biemans-Oldehinkel, E. & Poolman, B. (2003). On the role of the two extracytoplasmic substrate-binding domains in the ABC transporter OpuA. *EMBO J.* **22**, 5983–5993.
26. van Veen, H. W., Margolles, A., Muller, M., Higgins, C. F. & Konings, W. N. (2000). The homodimeric ATP-binding cassette transporter LmrA mediates multidrug transport by an alternating two-site (two-cylinder engine) mechanism. *EMBO J.* **19**, 2503–2514.
27. Schroers, A., Burkovski, A., Wohlrab, H. & Kramer, R. (1998). The phosphate carrier from yeast mitochondria. Dimerization is a prerequisite for function. *J. Biol. Chem.* **273**, 14269–14276.
28. Booth, I. R. (1985). Regulation of cytoplasmic pH in bacteria. *Microbiol. Rev.* **49**, 359–378.
29. Heuberger, E. H. M. L., Veenhoff, L. M., Duurkens, R. H., Friesen, R. H. E. & Poolman, B. (2002). Oligomeric state of membrane transport proteins analyzed with blue native electrophoresis and analytical ultracentrifugation. *J. Mol. Biol.* **317**, 591–600.
30. Yanisch-Perron, C., Vieira, J. & Messing, J. (1985). Improved M13 phage cloning vectors and host strains: nucleotide sequences of the M13mp18 and pUC19 vectors. *Gene*, **33**, 103–119.
31. Ebricht, R., Dong, Q. & Messing, J. (1992). Corrected nucleotide sequence of M13mp18 gene III. *Gene*, **114**, 81–83.
32. Wertman, K. F., Wyman, A. R. & Botstein, D. (1986). Host/vector interactions which affect the viability of recombinant phage lambda clones. *Gene*, **49**, 253–262.
33. Pourcher, T., Bibi, E., Kaback, H. R. & Leblanc, G. (1996). Membrane topology of the melibiose permease of *Escherichia coli* studied by melB-phoA fusion analysis. *Biochemistry*, **35**, 4161–4168.

Edited by I. B. Holland

(Received 26 January 2005; received in revised form 21 April 2005; accepted 22 April 2005)